ELSEVIER

Thin Solid Films 273 (1996) 116–121

thin solid films

UFM observation of lattice defects in highly oriented pyrolytic graphite

K. Yamanaka

Mechanical Engineering Laboratory, Namiki 1-2, Tsukuba, Ibaraki 305, Japan

Abstract

Ultrasonic force microscopy (UFM) can be used to image the distribution of elastic modulus up to several tens of GPa, which is not possible by the force modulation mode using a soft cantilever of spring constant less than 1 N m^{-1}. It was shown that by careful design of a piezoelectric transducer, together with a sample with small friction force, deflection vibration of the cantilever without torsion vibration is achieved, even during scanning perpendicular to the cantilever axis. Using this UFM, we propose that we have observed lattice defects reproducibly under atomically flat terraces of highly oriented pyrolytic graphite. Some defect was bent at surface steps, suggesting an interaction between the defect and the steps. The depth of a defect was found to be more than 3 nm on an assumption that it is continuous across surface steps. Contrast at the edge of terraces was explained by an geometrical effect associated with excitation of torsion vibration.

Keywords: Lattice parameters; Graphite; Pyrolysis

1. Introduction.

For material characterization in the nanometer scale, atomic force microscopy (AFM) was developed [1] and extended to observe elastic properties in force modulation mode [2,3]. In the force modulation modes a sample of AFM is vibrated and resultant cantilever deflection vibration is measured and used to produce elasticity images of objects. We have developed the lateral force modulation AFM (LM-AFM) [4–6] that measures a friction force amplitude and phase in real time and suppresses the cross talk from topography. However, in the force modulation modes, it is difficult to observe elasticity distribution and subsurface features of rigid objects, such as metals and ceramics using a soft cantilever.

When the sample is vertically vibrated at ultrasonic frequencies much higher than the cantilever resonance frequency, the tip cannot significantly vibrate due to the inertia of the cantilever. However, by modulating the amplitude of the ultrasonic vibration, the deflection vibration of the cantilever at the modulation frequency is excited due to the rectifier effect of the non-linear force curves [7,8]. Based on the tip–sample indentation during ultrasonic vibration, we developed ultrasonic force microscopy (UFM) for contact elasticity and subsurface imaging of rigid objects using a soft cantilever with a stiffness of the order of 0.1 N m^{-1} [9,10].

In this paper, we present results of analysis on the measurable range of elastic modulus in UFM. Then, we describe a transducer design, avoiding unwanted excitation of lateral vibration of the sample. Using this set-up, we realized deflection vibration without crosswalk of torsion vibration. Finally, we present comparison between surface topography and subsurface lattice defects in highly oriented pyrolytic graphite (HOPG) in some detail, as an extension of a previous report [9].

2. Elasticity measured by force modulation mode and UFM

To compare the measurable range of elasticity in the force modulation mode and UFM, we first summarize the analysis of force modulation mode using Hertzian contact model [2]. The contact radius is expressed as

$$A=\left(\frac{RF}{E^*}\right)^{1/3} \tag{1}$$

where, R is tip radius, F is contact force and

$$E^*=\frac{4}{3}\left[\frac{1-\nu_1^2}{E_1}+\frac{1-\nu_2^2}{E_2}\right]^{-1}$$

is the effective elasticity. The depth of indentation is given as

$$d=A^2R \tag{2}$$

From Eqs. (1) and (2),

$$d^3=\frac{A^6}{R^3}=\frac{R^2F^2}{R^3E^{*2}}=\frac{F^2}{RE^{*2}} \tag{3}$$

SSDI 0040-6090(95)06802-3

Differentiating by d and substituting contact stiffness defined as $s \equiv \partial F/\partial d$, it is shown that

$$E^* = \left(\frac{8s^3}{27RF}\right)^{1/2} \tag{4}$$

To determine the contact stiffness s experimentally, the force balance between the cantilever restoring force and the tip–sample force expressed as

$$kz_c = s(z_s - z_c) \tag{5}$$

is used, where k is the cantilever spring constant, z_c is cantilever deflection, and z_s is stage displacement. Using Eq. (5), Eq. (4) is rewritten as

$$E^* = \left(\frac{8k^3}{27RF}\right)^{1/2}\left(\frac{\gamma}{1-\gamma}\right)^{3/2} \tag{6}$$

where $\gamma \equiv z_c/z_s$ is a relative cantilever deflection divided by the stage displacement. This γ is the quantity to be measured experimentally.

Fig. 1(a) shows effective elasticity against relative cantilever deflection for a typical condition of contact mode AFM calculated using Eq. (6). The cantilever spring constant is 0.2 N m^{-1}, the tip radius is 20 nm and the normal force is 8 nN. Closed circles show rough estimate of E^* for typical materials. It is seen that a change of γ between soft organic materials with E^* of 0.01 and rigid organic materials with E^* of 1 GPa is large enough to be measured. However, change of γ among rigid materials with E^* ranging from 5 GPa to 100 GPa is too small to be measured. In attempts to measure rigid materials, a very stiff cantilever has to be used [3].

For UFM we have published a scheme for numerical calculation of the characteristics of the cantilever deflection [10]. Due to the non-linear characteristics, the cantilever deflection is not proportional to the stage displacement. Fig. 1(b) shows an additional cantilever deflection caused by the ultrasonic vibration of a sample as a function of the sample vibration amplitude. The same parameters were used as in Fig. 1(a). It is seen that E^* between 1 GPa and 50 GPa produces an easily measurable change of the additional cantilever deflection when the sample vibration amplitude is larger than 0.5 nm. Since E^* of industrial carbon and graphite ranges between 3.5 to 28 GPa they are expected to be suitable objects of UFM, as will be shown below.

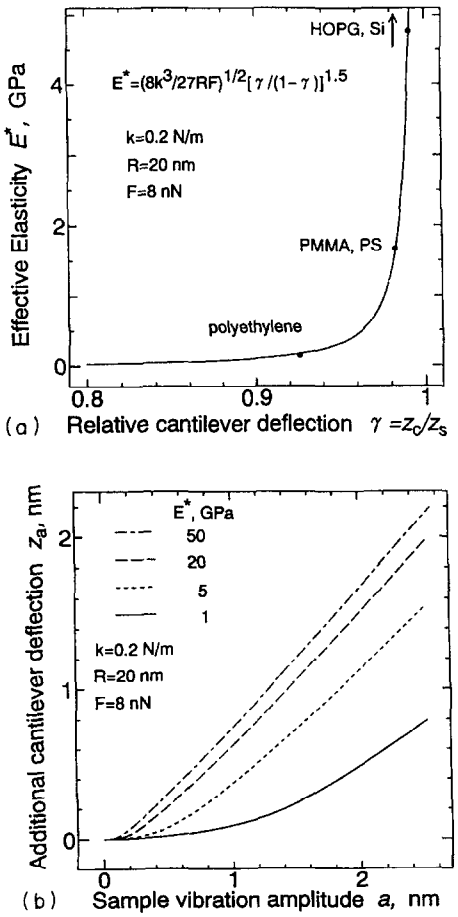

Fig. 1. Measurable range of elasticity in force modulation mode and UFM. (a) Relation between effective elasticity and relative cantilever deflection measured in the force modulation mode. Closed circles indicate typical values for some materials. (b) Additional cantilever deflection as a function of sample vibration amplitude measured in UFM.

3. Experimental details

Fig. 2 illustrates an UFM constructed based on an AFM/FFM system using the optical-beam-deflection sensor (Seiko Instrument Inc., SPI 3700). The sample is placed on a piezoelectric tube scanner used for four-fold purposes: x–y scanning for imaging, z-position control for the constant force mode, z-position translation. The normal force between the sample and a sharp tip supported by a soft cantilever is monitored from the vertical position of a laser beam at a four-

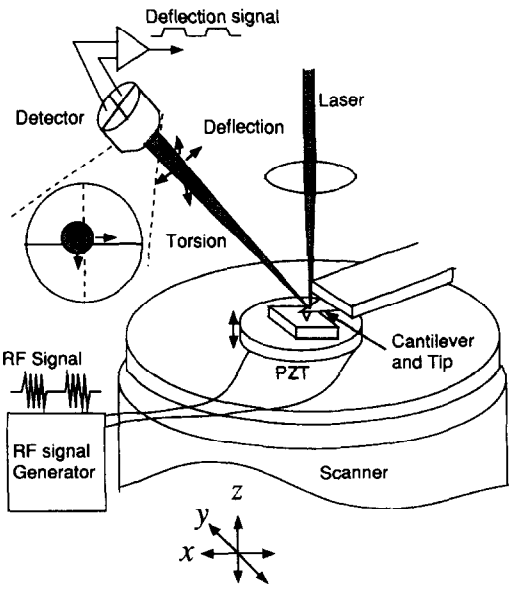

Fig. 2. Structure of the ultrasonic force microscope (UFM).

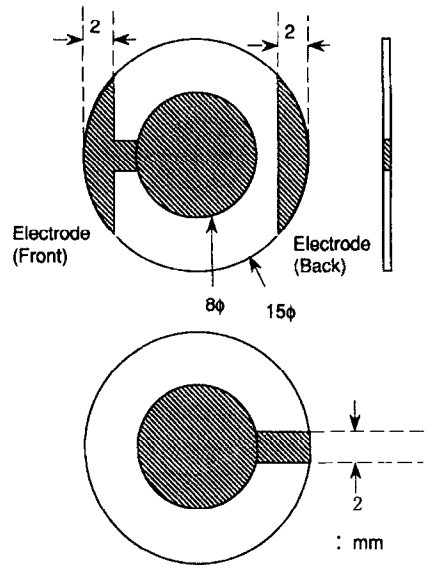

Fig. 3. Thickness-extension vibration PZT transducer used in the present UFM. The small electrode traps the energy in central region and suppress unwanted vibration of shear type.

segment photodiode (PD) reflected by the upper surface of the cantilever. The lateral force between the sample and the tip is monitored from the horizontal position of the laser beam at the PD. To excite ultrasonic frequency vibration in MHz range, a thickness-extension mode PZT piezoelectric transducer (Tokin PZT N-6) with a center frequency of 6.4 MHz was bonded on a sample stage and driven by a radio frequency (r.f.) signal generator. Fig. 3 shows a transducer design based on energy trapping vibration [11], where the diameter of the electrodes is much smaller than the diameter of the piezoelectric disk, and unwanted vibration modes of shear type are suppressed. Such a thickness-extension mode vibration without unwanted shear vibration is required to eliminate lateral vibration component of the sample that causes cantilever torsion vibration. A silicon nitride cantilever with a spring constant of 0.09 N m^{-1} and a silicon nitride tip was used.

A highly oriented pyrolytic graphite (HOPG) sample was purchased from Union Carbide (ZYH-Grade). The quality of the sample is classified according to mosaic spread, and mosaic spread of this sample was $3.5 \pm 1.5°$, which indicates considerable amount of defects. The sample was bonded to the PZT transducer with a phenyl salicylate ("zarol") frequently employed in ultrasonic measurements, and was cleaved in air just before the experiment.

4. Results and discussion

4.1. Deflection and torsion vibration signal

Fig. 4 shows oscilloscope traces of r.f. signal (upper), deflection signal (middle) and torsion signal (bottom) when

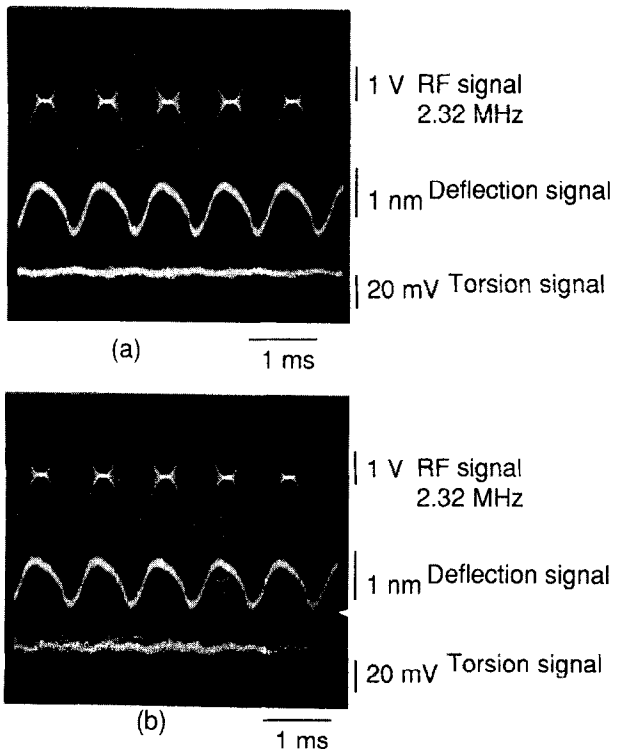

Fig. 4. Oscilloscope traces of driving signal (upper trace), deflection signal (middle trace) and torsion signal (bottom trace). (a) Signals observed with no scanning. (b) Signals observed during y scanning.

the y scanning was stopped (a), and during the y scanning with scan velocity of 2 mm s^{-1} (b). It is shown from Fig. 4(a) that deflection vibration at 1 kHz was clearly excited with good signal to noise ratio. If the PZT has a unwanted shear vibration in the y direction, a torsion signal will also be observed, but actually there was no vibration in the torsion signal. It shows a good performance of the transducer and a bonding between sample and transducer.

During the y scanning perpendicular to the cantilever axis, the cantilever torsion would be induced if the friction force is large. Then, the vertical ultrasonic vibration of the sample produces a torque for cantilever torsion. Consequently, torsion vibration of the cantilever at the modulation frequency would be excited, even though there is no lateral component of the sample. However, torsion vibration was not observed for the most part in the oscilloscope trace in Fig. 4(b). It indicates that friction force in HOPG is very small as described in Ref. [12].

Though the complementary use of deflection and torsion signal on a sample with a certain level of friction force is possible, careful evaluation of the two signals is required [9,10]. It should be noted that, without such a care, misleading interpretation of the UFM images might be derived. Therefore, in this paper, we deal with a sample with very small friction force, where it is justified to employ only the deflection signal. Torsion vibration occasionally excited as indicated by an arrow head in the bottom trace of Fig. 4(b) is regarded as an edge effect and will be discussed in Section 4.4.

4.2. Topography and subsurface defects in HOPG

The AFM height image shown in Fig. 5(a) was obtained at constant force of 0.1 nN in air (20 °C, 43% relative humidity), but due to the meniscus force, actual contact force was around 10 nN. It shows cleavage steps and the terraces between them, which are atomically flat. As shown in the surface profile in Fig. 5(c), some step height was 0.37 nm consistent with the inter layer distance of 3.35 A.

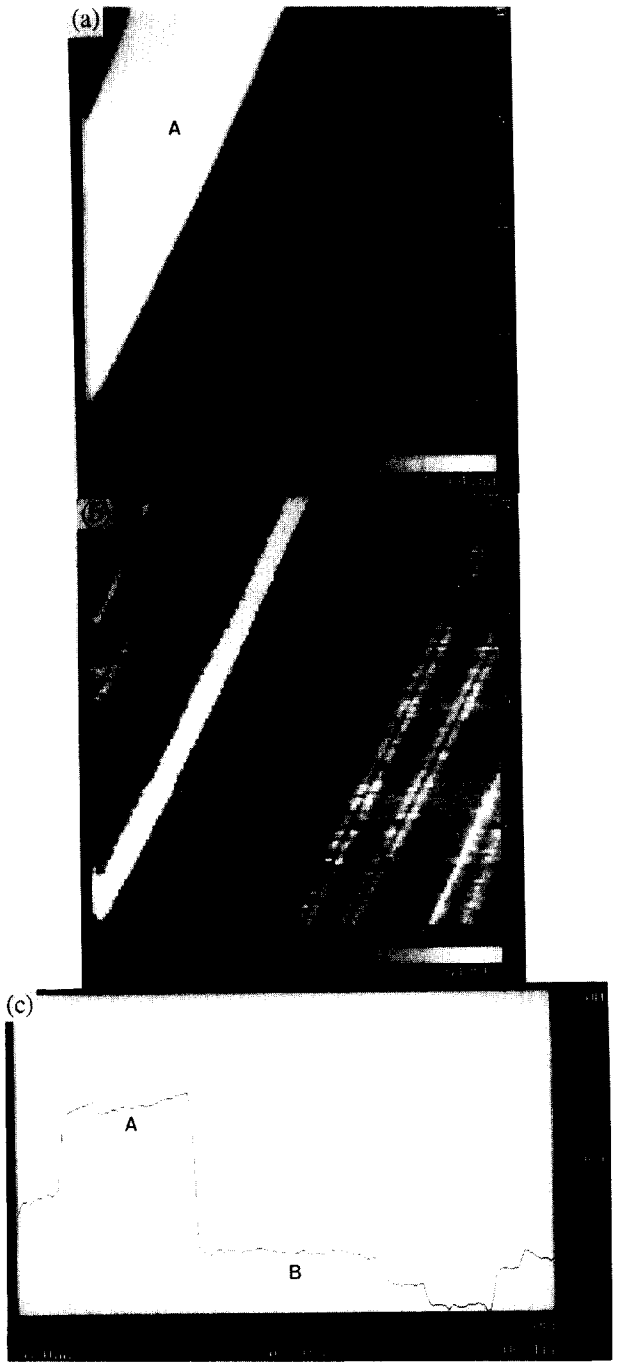

Fig. 5. Images of HOPG. (a) AFM height image. It shows cleavage steps and the terraces between steps are atomically flat. (b) UFM image obtained at 2.32 MHz. Continuous dark stripes indicated by an arrow head are observed. (c) Surface profile at the top of image (a). Some steps are of monolayer height and height difference between the terraces A and B is 3 nm.

A UFM image (Fig. 5(b)) was obtained from cantilever deflection vibration at 1 kHz with the sample vibrated at 2.32 MHz, with amplitude modulation at 1 kHz. Continuous dark stripes were clearly observed extending from the left upper corner to the right bottom corner as indicated by an arrow head. The amplitude of cantilever deflection vibration was a few percent smaller on the stripes than on the other area, showing lower elasticity. It is reasonable to assume that a stripe corresponds to an boundary of an extra half plane, i.e. edge dislocation, since the elasticity is expected to be low at such a boundary with a large inter atomic distance. Though another possibility cannot be ruled out that they are boundary of interstitial intercalation, i.e. foreign atoms or molecules adsorbed between atomic layers, similar discussion can be made regarding the elasticity. Then we tentatively assume that they are dislocations in this paper.

If the dislocations are further assumed to be continuous across the step between terraces A and B, the depth of the dislocation from surface of terrace A should be larger than 3 nm, since terrace A is 3 nm higher than terrace B. A model which explains this assumption is illustrated in Fig. 6. It is also noted that the dislocation is slightly bent at the step between terraces A and B, suggesting some interaction between the dislocation and the step.

On the other hand, the dislocations were not observed in topography images. This is reasonable since, according to Fig. 1(a), variation of elasticity in rigid objects will not make a detectable change in the cantilever deflection, if we use a soft cantilever with a spring constant around 0.1 N m^{-1}. Similarly, it was previously shown that the force modulation mode produces no image contrast that suggests a subsurface feature in HOPG [9].

Fig. 7(a) and 7(b) show friction force microscope (FFM) images of the same sample, and it is seen that there is no friction force variation on the terraces except the neighborhood of steps. It is reported that crystal planes of different orientations from (0001) and amorphous carbon region sometimes emerged on cleaved surface of HOPG where the friction forces are more than an order of magnitude larger

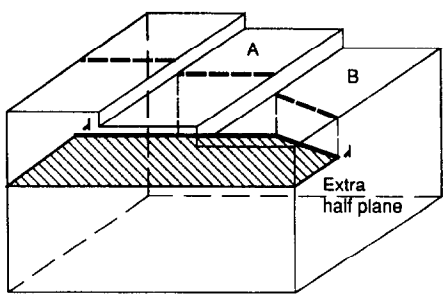

Fig. 6. Schematic illustration of an edge dislocation (thick solid lines) which is a boundary of an extra half plane. Thick broken lines are projection of the dislocation to the surface. It is bent at a surface step between terraces A and B.

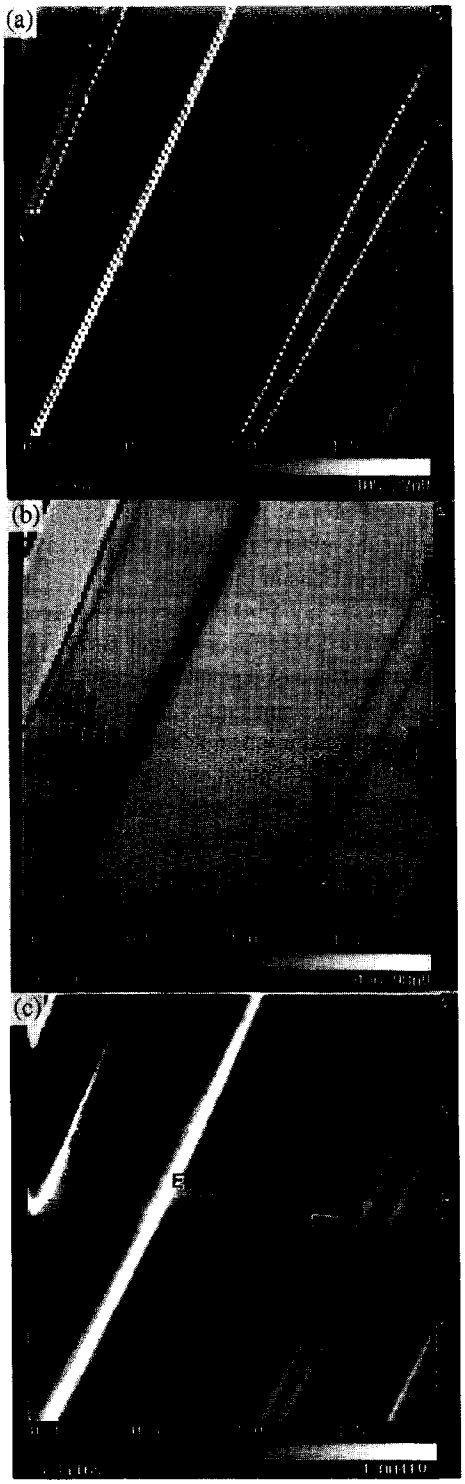

Fig. 7. (a) and (b) Friction force microscope images at forward and reverse y scanning. (c) UFM image obtained at 2.32 MHz. Three continuous subsurface defects were observed. A kink is observed on only one of them at the intersection point with a surface step, as indicated by an arrow head.

than (0001) surface [12]. However, the present FFM image rules out such possibility.

On a UFM image (Fig. 7(c)), obtained at 2.32 MHz, three continuous dislocations were observed. These dislocations are extension of those observed at the left upper corner in Fig. 5. Though they appear to occur in parallel multiples, it is not due to the artifacts such as the multi-tip effect, but they probably correspond to individual dislocations. In fact, an interesting feature was observed in this image; one of the three dislocations has a kink at a position of a surface step indicated by an arrow head, whereas the other two are straight. Since no anomaly is observed in the FFM images, this kink seems to be a subsurface feature. This fact indicates that one of the three dislocations interacted with the surface step.

4.3. Advantage of UFM

Investigation of dislocation behavior on the nanometer scale has so far been carried out mostly using the transmission electron microscopes, (TEM) [13]. However, TEM requires a very thin sample and the thinning process is not easy. In contrast, UFM does not require such a thinning process. Furthermore, interaction of dislocations with surface steps is not possible to observe with TEM, since TEM produces information averaged through the depth. In contrast, precise surface topography is obtained in UFM when the ultrasonic vibration is switched off. It is because the soft cantilever used in UFM eliminates a problem of sample deformation, sometimes encountered when using a rigid cantilever. Consequently, a monolayer step was clearly observed, as seen in Fig. 5(a) and 5(c). Therefore, it was demonstrated that UFM is a quite attractive tool for investigating lattice defects together with topographic information.

It is known that the a cleavage crack is modeled as collection of dislocations and there are cases where step formation takes place when a propagating cleavage crack plane interacts with dislocations [13]. Although these interactions are mostly conceptual ones and little experimental verification is available, present observation provides examples of such interactions. Though the mechanism of interaction observed in this work is not clear at this moment, further detailed study with UFM will reveal many interesting aspects of the behavior of lattice defects.

4.4. Edge effect

Finally, we comment on the origin of the bright stripes observed at the position of steps in UFM images, marked E, in Fig. 5(c) and 7(c). As pointed out in Section 4.1, torsion vibration was occasionally observed during the y scanning. At the same time the deflection vibration amplitude also increased, correspondingly, as shown by an arrow head in the middle trace of Fig. 4(b). It was found by monitoring the oscilloscope during the x–y scanning, that the bright stripe in images corresponds to this larger amplitude deflection signal. Since the large deflection amplitude accompanies a large torsion amplitude, the source of these large amplitude signal seems to be the large local gradient at steps. Then the bright stripe in UFM images at the position of steps is probably interpreted as an edge effect, where the surface gradient is large.

However, the width of the bright stripe was around 100–120 nm and seems rather too large in a condition with a step height of 3 nm and the tip radius of around 20 nm. The actual tip radius might be larger due to contamination or wear of the tip. This point will be investigated in the future.

5. Conclusions

By a careful design of a piezoelectric transducer, together with samples with small friction force, deflection vibration of cantilever without torsion vibration was realized, even during scanning perpendicular to the cantilever axis. We propose that we are detecting lattice defects like dislocation or intercalation reproducibly under atomically flat terraces of highly oriented pyrolytic graphite. Some defect was bent at surface steps and its depth was more than 3 nm on the assumption that it is continuous across surface steps. Contrast at the edge of terraces was explained by an geometrical effect associated with excitation of torsion vibration.

Acknowledgements

The author is very grateful to Dr. M. Kadota, Murata mfg. Co. Ltd. for helpful discussion on the energy trapping vibration.

References

[1] G. Binnig, C.F. Quate and Ch. Gerber, *Phys. Rev. Lett., 56* (1986) 930.
[2] M. Radmacher, R.W. Tillmann and H.E. Gaub, *Biophys. J., 64* (1993) 735.
[3] P. Maivald, H.J. Butt, S.A.C. Gould, C.B. Prater, B. Drake, J.A. Gurley, V.B. Elings and P.K. Hansma, *Nanotechnology, 2* (1991) 103.
[4] K. Yamanaka, O. Kolosov, H. Ogiso, H. Sato and T. Koda, *Proc. Jpn. Acoust. Soc. Spring Meeting*, 1993, p. 889.
[5] E. Tomita, K. Yamanaka and M. Fujihira, *Ext. Abstr. 41st Spring Meeting of the Jpn. Soc. Appl. Phys. and Related Societies, Tokyo*, 1994, 30a-MC-8, p. 446.
[6] K. Yamanaka and E. Tomita, Ext. Abstr. 55 th Autumn Meeting of the Japan Soc. Appl. Phys. Nagoya, September, 1994, 21p-Q-2, p. 456, *Jpn. J. Appl. Phys.*, (1995).
[7] W. Rohrbeck and E. Chilla, *Phys. Status Solidi (a), 131* (1992) 69.
[8] O. Kolosov and K. Yamanaka, *Jpn. J. Appl. Phys., 32* (1993) L1095.
[9] K. Yamanaka, H. Ogiso and O. Kolosov, *Appl. Phys. Lett., 64* (1994) 178.
[10] K. Yamanaka, H. Ogiso and O. Kolosov, *Jpn. J. Appl. Phys., 33* (1994) 3197.
[11] R. Beckmann, *Proc. IRE, 49* (1961) 523.
[12] J.-A. Ruan and B. Bhushan, *J. Appl. Phys., 76* (1994) 8117.
[13] A.S. Tetelman and A.J. Mcevily, Jr., *Fracture of Structural Materials*, Wiley, New York, 1967.